

Influence of turbine blades fabrication conditions on their lifetime

M. SOHACIU, S. CIUCĂ*, D. SAVASTRU^a, G. COMAN, A. PREDESCU, A. BERBECARU, C. COTRUȚ, E. MATEI, I. A. GHERGHESCU, C. PREDESCU

Politehnica University of Bucharest, Romania

^aNational Institute of R&D for Optoelectronics INOE 2000, 409 Atomistilor Street, PO BOX MG-5, RO 077125, Magurele – Ilfov, Romania

The paper presents results of research regarding the behavior in time of the material used in the construction of two hydroelectric turbines on the river Olt.

The optoelectronic methods and other techniques of investigation were used:

- Metallographic analysis by optical microscopy;
- Structural and compositional investigation by scanning electron microscopy and energy dispersive spectrometry
- Estimation of corrosion resistance by electrochemical experiments

The elaboration and casting process of the used martensitic stainless steels are decisive elements concerning the lifetime of the two hydroelectric turbines.

(Received October 28, 2015; accepted April 5, 2016)

Keywords: Turbines manufacturing, Martensitic stainless steels, SEM, EDS, Corrosion resistance

1. Introduction

Turbines manufacturing for hydropower plants involves utilization of high quality martensitic stainless steels with fine homogeneous microstructures providing good mechanical properties and high corrosion resistance. The paper presents a comparison between two turbines, one made of G-X4CrNi13-4 steel from “CH 1 – Sample 1” with a corroded surface after two years of operation and another one made of T8NCuMC130 steel from “CH 2 – Sample 2” after twenty years of operation, but still having an acceptable condition [1, 2].

The corroded surface of the turbine blade realized from G-X4CrNi13-4 is shown in Fig. 1 and the other one, realized from T8NCuMC130, in Fig. 2.

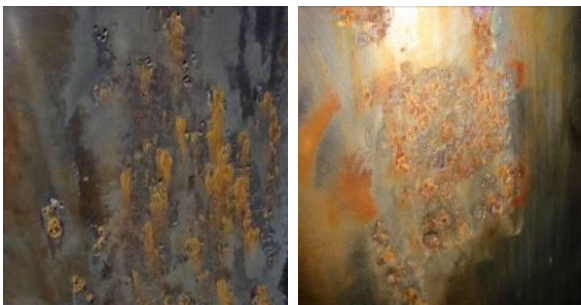


Fig. 1. Corroded surface of the turbine blade from “CH 1 - Sample 1”



Fig. 2. Surface of the turbine blade from „CH 2 - Sample 2”

The aim of our work is to explain the different corrosion behavior of the two analyzed turbines, both made of martensitic stainless steels. All observations will be focused on detailed studies regarding the structure. The electrochemical tests will complete the range of information concerning the relationship between chemical composition, structure and properties, generally valid for any material [3, 4].

2. Experimental researches and discussion

The investigations are conducted respecting the following steps:

- **Determination of chemical composition** using optical emission spectroscopy, realized with LECO spectrometer;
- **Determination of material hardness**, using MIC 20 Krautkramer microhardner;
- **Metallographic analysis by optical microscopy** using a Leica metallographic microscope with equipment for photo capture;

- **Microstructure and micro-composition analysis** by scanning electron microscopy (SEM) and energy dispersive X ray microanalysis using Quanta Inspect F microscope;

- **Estimation of corrosion resistance** by Electrochemical experiments, carried out with a PARSTAT 4000 potentiostat/galvanostat (Princeton Applied Research, USA) associated to a low current box (VersaSTAT LC, Princeton Applied Research, USA). The potentiodynamic curves were acquired with a VersaStudio v.2.43.3 software.

Samples were collected in-situ from the two turbines: CH 1 – Sample 1 (Fig. 1) and CH 2 – Sample 2 (Fig. 2).



Fig. 3. The region where the samples were taken from the turbine CH 1 – Sample 1

The resulted chemical composition is indicated in Table 1.

Table 1. Chemical composition of the steels

Elements, %	CH Frunzaru turbine blade, sample 1	G-X4CrNi13-4 ASTM A743/A743M (2003) CA6NM	CH Izbiceni turbine blade sample 2	T8NCuMC130 CS L03.009.0 CCSIT Reșița
C	0.025	<0.06	0.074	max.0.1
Si	0.4	<1	0.332	max.0.4
Mn	0.73	<1	0.595	0.2÷0.6
P	0.035	<0.035	0.016	max.0.025
S	0.002	<0.025	0.022	max.0.03
Cr	12.6	12÷13.5	13.453	12÷13.5
Mo	0.35	0.4÷1	0.066	-
Ni	3.82	3.5÷4.5	1.325	1÷1.5
V	0.03	-	0.029	-
Al	0.012	-	0.011	-
Cu	0.35	-	1.295	1÷1.3

As shown, in both cases the chemical composition is framed in the standardized norms [5].

Measuring for hardness tests has been realized on the sample surface coming from the turbine blade CH1 - Sample1 and CH 2 - sample 2. The values are presented in Table 2.

Table 2. Values of hardness HV10 for the two studied steels

No.	Sample name	Measured values	Average value
1	CH 1 turbine blade Sample 1	284; 283; 291	286
2	CH2 old turbine blade Sample 2	250; 235; 241	242

Microstructure resulted by Optical Microscopy

The aim of the metallographic analysis was to investigate the inclusional state of the two types of materials and confirm the quenched and tempered structure recommended in all situations for the martensitic stainless steel. Thus, the prepared and unetched samples indicate in the case of sample 1 a generalized presence of some discontinuities in the bulk of material with circular and/or elliptical shape with variable dimensions, associated with a dense inclusions dispersion. The inclusions and discontinuities are randomly oriented (Fig. 4).

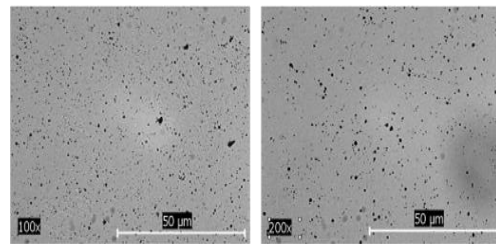


Fig. 4. Metallographic microstructure on unetched sample 1

In the case of sample 2 the inclusional state and material discontinuities are more rare, suggesting a suitable casting process.

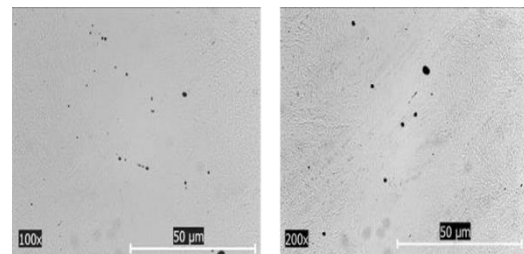


Fig. 5. Metallographic microstructure on unetched sample 2

In order to observe the quenched and tempered structure, the samples were etched with Mable’s reagent and examined again by optical microscopy.

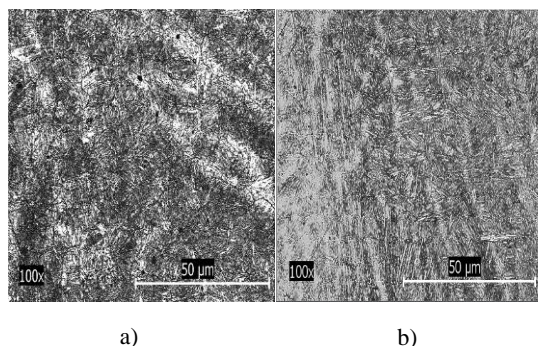


Fig. 6. Metallographic microstructures on etched samples (Marble's reagent) a) Sample 1; b) Sample 2

The metallographic structure is typical for a martensitic stainless steels quenched and tempered. Both steels reveal an uniform distribution of sorbite with hardness values (286 HV for sample 1, respectively 242 HV for sample 2) in conformity with the obtained structure. This information demonstrates a correct technology of the heat treatment [6].

Microstructure and micro-composition resulted by SEM and EDS

The microstructures and microcompositions of the analyzed samples by scanning electron microscopy and energy dispersive spectrometry underline the nature and size of the observed inclusions by optical microscopy.

Fig. 7 shows a SEM image associated with local chemical composition, performed on sample 1 in a microarea where a discontinuous oxidic network with angular dispersed particles has been detected [7]. The local chemical composition data affirm that these oxides are rich in aluminium.

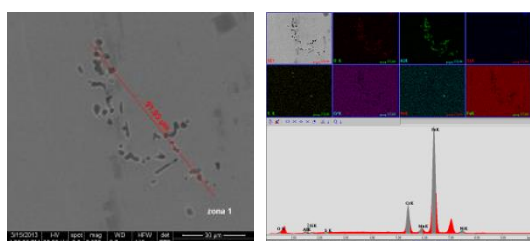


Fig. 7. SEM and EDAX of sample 1; micro-area with a network of inclusions rich in aluminium oxides

Fig. 8 shows the record of another field in sample 1 with some particles having rounded shapes and some particles with angular distribution [8]. The results of local chemical composition demonstrate that in this zone there is a complex inclusional state: sulphides (MnS), more plastic justifying the rounded distribution and oxides (rich in aluminium and silicon), more fragile with angular shapes.

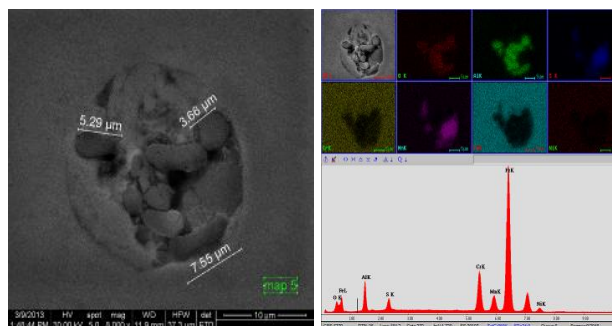


Fig. 8. SEM and EDAX of sample 1 micro-area with complex inclusions rich in aluminium and silicon oxides and sulphides (MnS)

The Fig. 9 represents a micro-area of sample 2. It is obvious to observe that the quality of the surface is superior, compared to sample 1, even though some dispersed inclusions exist. The micro-chemical analysis have highlighted its character, emphasizing that they are sulphides (type of MnS).

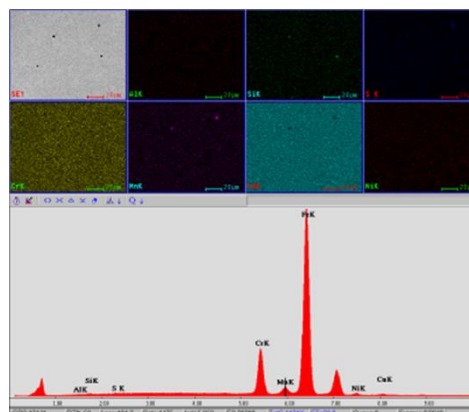


Fig. 9. SEM and EDAX of sample 2 micro-area with sulphides (MnS) inclusions

The obtained results by chemical and structural observations are very suggestive, demonstrating that the inclusional state of the steels decisively influences the behavior in working. The electrochemical tests will lead to concrete information on the corrosion resistance, one of the main characteristics of the turbine blades.

Estimation of corrosion resistance

The corrosion behavior of the samples was studied using electrochemical techniques in saline solution NaCl 3.5% at a temperature of 25°C. The tests were performed in a three electrode corrosion cell made of a saturated calomel electrode (SCE) as reference electrode, a platinum counter electrode and the working electrode consisting in the tested samples. These were metallographic prepared,

because any unevenness of the surface influences the corrosion behavior [9, 10, 11, 12].

The corrosion resistance was determined by the Tafel technique. Tafel plots allow the direct measurement of the corrosion current from which the corrosion rate can be quickly calculated. This method consists in plotting the linear polarization curves, respectively plotting the potentiodynamic polarization curves between -250 mV (vs OCP) and $+250$ mV (vs OCP). The scanning rate was of 1 mV/s.

The resulted Tafel curves are presented in Fig. 10. For a better understanding, these were superposed.

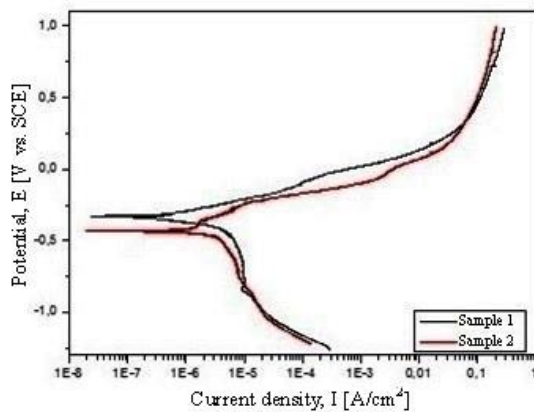


Fig. 10. Tafel curves for samples 1 and 2 in saline solution NaCl 3.5% at the temperature of 25°C

In order to estimate the corrosion resistance of the investigated samples, the following parameters were determined from the Tafel curves: the corrosion potential (E_{corr}), the corrosion current density (i_{corr}), the cathodic curve slope – Tafel constant β_c , the anodic curve slope – Tafel constant β_a .

Their values allowed the calculation of the parameters that describe the tested samples corrosion resistance: corrosion rate (CR) and polarization resistance (R_p).

Table 3 shows the main parameters of the electrochemical corrosion process.

Table 3. Main parameteres of the corrosion process

Sample	1	2
E_{cor} (V)	-431.666	-331.157
i_{cor} ($\mu\text{A}/\text{cm}^2$)	3.806	1.528
CR ($\mu\text{m}/\text{y}$)	42.631	17.298
β_c (mV)	231.918	310.66
β_a (mV)	961.595	214.887
R_p ($\text{k}\Omega\text{cm}^2$)	21.34	36.14

The formula for calculating the corrosion rate, according to ASTM G102-89 (2004), is the following:

$$CR = K_i \cdot \frac{i_{\text{corr}}}{\rho} \cdot EW \quad (1)$$

where: CR is the corrosion rate (mm/year), K_i is a constant, 3.27×10^{-3} , ρ is the alloy density (g/cm^3), i_{corr} is the corrosion current density (nA/cm^2) and EW the equivalent weight (g).

Polarization resistance was determined according to ASTM G59-97 (2003) with the formula:

$$R_p = \frac{1}{2.3} \cdot \frac{b_a b_c}{b_a + b_c} \cdot \frac{1}{i_{\text{corr}}} \quad (2)$$

where: β_a is the anodic curve slope, β_c is the cathodic curve slope and i_{corr} the corrosion current density (nA/cm^2).

The samples corrosion resistance was estimated according several evaluation criteria.

Considering the corrosion potential (E_{corr}), a higher electropositive value denotes a better corrosion behavior in the chosen medium, our case being standard saline solution. When examining the resulting values of E_{corr} , we can notice that sample 2 has a higher electropositive value ($-331,157$ mV), by comparison with sample 1 ($-431,666$ mV). In the same time, a low value of the corrosion current density (i_{corr}) suggests a higher corrosion resistance. Hence considering this criterion, the best corrosion behavior is displayed by the sample 2 too, with an i_{corr} value of $1,528 \mu\text{A}/\text{cm}^2$, compared to i_{corr} value of $3,806 \mu\text{A}/\text{cm}^2$ of the sample 1.

Another widely known fact is that a high polarization resistance (R_p) reveals a good corrosion behavior and a low value of this parameter gives evidence of an unsatisfactory behavior in corrosive media. In this case too, sample 2 show higher values of polarization resistance comparing to sample 1. After calculating the corrosion rate (CR) in standard saline solution for both samples, one can see that the lowest value is obtained for the sample 2 ($17.298 \mu\text{m}/\text{year}$), the sample 1 having a higher value ($42.631 \mu\text{m}/\text{year}$).

Taking into account all these observations, it becomes easy to observe better corrosion behavior of the sample 2.

3. Conclusions

The chemical composition of the steels corresponds to the standardized norms: sample 1, *GX4CrNi13-4 EN 10283*, or *ASTM A743/A743M(2003) CA6NM* and sample 2 *T8NCuMC130 CS L03.009.0 CCSIT Resita*. All of them are martensitic stainless steels and recommended to be used for hydraulic turbine blades.

Metallographic structure resulting by optical microscopy on samples taken from both steels and etched with Marble's reagent reveals a sorbitic uniform distribution. The structure is typical for a martensitic stainless steels quenched and tempered and demonstrates a correct technology of the heat treatment.

Examination by optical microscopy, but on unetched samples, indicates an inclusional state and material discontinuities totally different for the two sample. For the

sample 1 discontinuities are present in the overall mass of the material with circular and / or elliptical sizes and a large density of non-metallic inclusions. For the sample 2, the discontinuities are unobservable and the inclusions are distributed in small areas.

Analysis by SEM and EDS techniques leads to more concrete results concerning the inclusions chemical composition. In the sample 1, the inclusions are sulphides (MnS) and oxides (rich in aluminium and silicon), while in the sample 2 these are only sulphides (MnS). No oxides have been detected here.

The presence of sulphide and oxide inclusions represent a risk factor for localized pitting or crevice corrosion, specific for the stainless steel whose surface is passivated by a protective oxide layer. Passivated surface is the cathode and the anode becomes the existing inclusion, locally creating micro-galvanic cells and initiating the corrosion process.

The results of electrochemical tests are in accordance with the structural observations, demonstrating that the steel whose structure is more correct after casting has the better corrosion resistance.

Even if the steel G-X4CrNi13-4, in conformity with chemical composition, is theoretically superior to the steel T8NCuMC130, the corrosion behavior of the second was much better. We appreciate that the most important source of corrosion was the quality of material (inclusions, discontinuities) resulting from the elaboration and casting process.

Acknowledgement

The work has been funded by the Sectoral Operational Programme "Increase of Economic Competitiveness", ID 1799/SMIS 48589/2015.

References

- [1] A. Buzăianu, P. Moțoiu, I. Csaki, G. Popescu, K. Ragnarstottir, S. Guðlaugsson, Daniel Guðmundsson, Adalsteinn Arnbjornsson, *Geothermics*, 57 (2015).
- [2] M. Sohaciu, C. Predescu, E. Vasile, E. Matei, D. Savastru, A. Berbecaru, *Dig J Nanomater Bios* 8(1), 367 (2013).
- [3] V. Geanta, I. Voiculescu, R. Ștefanioiu, D. Savastru, D. Daisa, *J. Optoelectron. Adv. M.* 15(11-12), 1457 (2013).
- [4] C. Predescu, N. Ghiban, M. Sohaciu, D. Savastru, E. Matei, A. Predescu, A. Berbecaru, G. Coman, *Optoelectron. Adv. Mat.* 8(1-2), (2014).
- [5] V. Geanta, M. Taca, D. Daisa, I. Voiculescu, R. Ștefanioiu, D.M. Constantinescu, D. Savastru, J. *Optoelectron. Adv. M.* 17(7-8), (2015).
- [6] M. I. Rusu, R. Zamfir, E. Ristici, D. Savastru, C. Talianu, S. Zamfir, A. Molagic, C. Cotrut, J. *Optoelectron. Adv. M.*, 8(1), 230 (2006).
- [7] John Kuo, *Electron Microscopy. Methods and Protocols-Second Edition-2nd*, Center for Microscopy and Microanalysis, Crawley, Australia, (2007).
- [8] Zhigang R. Li, *Industrial Applications of Electron Microscopy*, DuPont Company, Wilmington, Delaware, U.S.A., (2003).
- [9] N. Chermat-Aourasse, R. Kesri, *Protection of Metals*, 43(4), 344, 2007L.
- [10] R. Godec, V. Doleček, *Materials and Corrosion*, 45(9), 517 (1994).
- [11] S. Hashizume, Y. Minami, Y. Ishizawa, *Corrosion*, 54(12), 1003 (1998).
- [12] A. E. Chivu, S. Ciuca, D. Bojin, F. S. Fedorov, A. Gebert, J. Eckert, *UPB Sci. Bull. Series B*, 47(4), 249, (2012).

*Corresponding author: sorin.ciuca@upb.ro